The local environment of Dy^{3+} in selenium-rich chalcogenide glasses.

Emma Barney[1], Zhuoqi Tang[1], Angela Seddon[1], David Furniss[1], Slawomir Sujecki[1], , Trevor Benson[1], Nigel Neate[1] and Diego Gianolio[2]*

[1] Faculty of Engineering, University of Nottingham, University Park, Nottingham, NG7 2RD

[2] Diamond Light Source, Harwell Science and Innovation Campus, Fermi Ave, Didcot, Oxfordshire OX11 0QX

*Corresponding author: Emma.Barney@nottingham.ac.uk

Abstract

The environment of Dy^{3+} is investigated when added as $DyCl_3$ or Dy foil into two base glasses, $Ge_{16.5}As_{19-x}Ga_xSe_{64.5}$, where x= 3 or 10 at.%, at doping levels between 0 and 3000 parts per million by weight (ppmw) Dy^{3+}. Extended X-ray Absorption Fine Structure demonstrates the glasses doped with Dy foil, or less than 1000 ppmw Dy^{3+} as $DyCl_3$, contain Dy ions that are fully incorporated into the glass network and are coordinated by 7-8 Se atoms. However, when the $DyCl_3$ dopant is present in concentrations ≥ 1000 ppmw Dy^{3+} the environment is dominated by Dy-Cl bonds. Furthermore, these Dy-Cl environments are nanocrystalline, retaining chemical order beyond the first coordination shell. By comparison with XRD and FTIR results, we report that the presence of α-Ga_2Se_3 crystallites in the glass, and the increased optical scattering in the fibres, are both related to the presence of $DyCl_3$ crystallites.

1. Introduction

Rare earth (RE) ion doped chalcogenide glasses are promising materials for active photonic devices operating in the mid-infrared (mid-IR). The mid-IR region, covering 3-25 µm, can be used for sensitive chemical analysis by exploiting the vibrational absorption bands exhibited by molecular species across this wavelength range. These bands exhibit large extinction coefficients and the spectra observed give “chemical fingerprints” that allow the presence and concentration of molecular species to be determined. Photonic devices based on these principles would have sensing applications in a wide range of fields including manufacturing, environmental monitoring [1], drug and explosives’ detection and identification [2], and medical applications [3].

To create a photonic sensing device that operates in the mid-IR, it is desirable to be able to produce mid-IR laser light in a compact, integrated device. The use of glass as a host for rare earth (RE) ions to create a lasing environment has been exploited extensively in the visible and near-infrared, for instance silica fibre lasers doped with ytterbium ions offer efficient high-power near-infrared fibre power sources [4]. The development of mid-IR fibre lasers would facilitate both imaging and chemical sensing but an alternative host to silica is required because silica fibres rapidly become opaque beyond 2 μm.

Chalcogenide glasses, which can transmit light from the far visible to wavelengths in excess of 15 μm, seem ideal candidates to develop as fibre lasers and to exploit mid-IR molecular absorptions for sensing applications. However, while a Raman laser has been demonstrated at 3.77 μm [5], success in creating a mid-IR rare earth fibre laser has, thus far, been limited and there are none available for general room temperature use operating beyond 3 μm [6]. Laser emission of Dy^{3+} at ~4.5 μm is close to the absorption band of Se-H bonds giving resonant absorption of the RE ion florescence, suppressing the lasing response desired [7]. To address this, significant effort has been made to develop purification methods for the constituent elements of chalcogenide glass [8,9]. Distillation methods for glasses have been used to produce simple composition chalcogenide fibres (no RE doping) with ultra-low loss [10] but, thus far, it has not been possible to eliminate completely hydrogen absorption bands from the glass.

Although the interaction of the RE ions with chalcogenide glass is not fully understood, there is evidence that the RE does not always bond to the chalcogen anions and the presence of impurities such as oxygen can result in the formation of undesirable RE bonds that provide routes for non-radiative decay, rather than radiative emission of light [11]. The preference for RE ions to bond to impurity anions in the glass has been attributed to the high electropositivity of RE ions and the greater electronegativity of impurities such as oxygen and halogen atoms when compared to the resident chalcogen. Previous work by Tang *et al.* [12] provides evidence for this type of behaviour, suggesting that Dy^{3+} doped into $Ge_{16.5}As_9Ga_{10}Se_{64.5}$ (atomic (at) %) preferentially scavenges oxygen impurities in the glass. RE-O bonds increase the phonon energy of the local environment encouraging non-radiative decay rather than radiative emission. Therefore, the drive to produce very pure chalcogenide glasses is important to the development of efficient mid-IR fibre lasers. Impurity-free glasses are required to ensure that the doped RE ions are bonded to the chalcogen atoms in the glass network. The presence of a significant level of oxygen in chalcogenide glasses, as in Ga-La-S-O glass optical fibres, also has the effect of increasing the global phonon energy of the glass, limiting the maximum wavelength of light transmission and lasing [13].

The limited solubility of RE ions in chalcogenide glasses is a further factor which limits the development of a fibre laser [14]. When RE ions are present in significant quantities in any glass they appear to exhibit a tendency to cluster. Thus, ion-ion interactions, arising from two RE ions in close proximity, act to depopulate the excited state and quench luminescence. Moreover, physical clustering may lead to phase separation and devitrification. Work by Aitken *et al.* has shown that the addition of 1.7 at.% Ga to a glass with composition $Ge_{25}As_{10}S_{65}$ (at%) increased the amount of RE that could be doped into the glass from ~200 ppm to 5000 ppm [14]. Furthermore, a comparison of the fluorescence from $Ge_{25}As_{10}S_{65}$ and $Ge_{25}As_{9.8}Ga_{0.2}S_{65}$ (at%), when both were doped with 450 ppm Pr^{3+}, showed an order of magnitude increase in the Pr^{3+} fluorescence intensity at 1350 nm in the Ga modified glass. The implication of this work is that the RE ions were more evenly dispersed throughout the chalcogenide glass network when Ga was present [14]. Aitken *et al.* suggest that this is due to a preference for Ga-S-RE linkages in the glass, and *ab initio* modelling of RE-doped sulfide glasses indicate that these linkages persist in the melt longer than Ge-S-RE [15].

The relationship between gallium and RE ions in chalcogenide glasses has been inferred from the fluorescence measurements [14], but there have been few direct structural studies to test the validity of the proposed Ga-S-RE complex. In large part, this is because diffraction measurements are not sensitive to the doping levels of RE ions required. EXAFS has been used as a probe, exploiting its element specificity and sensitivity. Choi *et al.* have reported that Dy^{3+} ions in a Ge-As-S glass are bonded with a coordination number of 6.7 ± 0.5 to sulfur with an average Dy-S bond length of 2.78 Å [16]. They report that the chalcogenide glass environment is more covalent than that found in crystalline Dy_2S_3. A second EXAFS study [17,18] has investigated Tm^{3+} doped sulfide glasses, xCsBr 1-x($Ge_{0.25}Ga_{0.10}S_{0.65}$ (at%)) and demonstrated that the RE ions preferentially bond to electronegative halogen ions in these chalcohalide glasses.

This paper is a continuation of work published by Tang *et al.* [11,12,19] and Seddon *et al*. [7] that have presented FTIR and X-ray diffraction data for a series of GeAsSe glasses modified with 3, or 10, at.% Ga and doped with differing concentrations of Dy^{3+} added as Dy foil or $DyCl_3$. The effect of varying both the glass composition [11,12], and the Dy precursor [19,20] has previously been investigated, and it has been shown that the Ga_{10} glasses doped with ≥ 1000 ppmw $DyCl_3$ exhibited α-Ga_2Se_3 crystals on melt-quenching [12]. No such crystallisation was observed in glasses of the same base glass composition doped with Dy foil [20]. It has been suggested by these Authors that the chloride precursor etches the SiO_2 ampoule used to contain the melt, introducing oxygen to the melt in addition to the oxygen-based impurities brought in with the precursors [12,20]. Furthermore, it has been suggested that the preferential association of Dy^{3+} with oxygen resulted in the formation

of Dy_2O_3 nanocrystallites that, in turn, acted as an heterogeneous nucleating agent for the α-Ga_2Se_3 crystals [11]. The variation in the Dy^{3+} environment with chalcogenide glass composition is of great interest for its effect on the lasing potential of the glass and any influence on the glass structure. This paper reports EXAFS spectra for a number of Dy^{3+}-doped $Ge_{16.5}As_9Ga_{10}Se_{64.5}$ and $Ge_{16.5}As_{16}Ga_3Se_{64.5}$ glasses, deliberately selected from those previously reported upon [7,11,12,19,20] to investigate the effects of Dy^{3+} doping level, Ga concentration, and the form of the Dy^{3+} precursor on the dysprosium environment. The results are then discussed in conjunction with previously reported FTIR and XRD results to develop a deeper understanding of the interaction of the Dy^{3+} with the glass network.

2. Experimental detail:

Nine samples have been included in this study, allowing the effects of dopant concentration, dopant precursor, and Ga content on the glass to be studied. Eight glasses have the base glass composition of $Ge_{16.5}As_9Ga_{10}Se_{64.5}$ (at%), seven of which were further doped with $DyCl_3$ at concentrations of 0, 500, 800, 1000, 1550, 2000 and 3000 ppmw Dy^{3+}; the remaining one was doped with 3000 ppmw Dy^{3+} as Dy foil. The final sample was a $Ge_{16.5}As_{16}Ga_3Se_{64.5}$ glass doped with 3000 ppmw Dy^{3+} as $DyCl_3$. Table 1 lists the nine glasses studied, and gives the abbreviated names for them that will be used to discuss the results.

2.1.Sample preparation

$Ge_{16.5}As_{(19-x)}Ga_xSe_{64.5}$ (atomic%), for x=10 and x=3 glasses were prepared by the melt-quenching method. High purity host glass elements: Ge (5N, Cerac), As (7N, Furukawa Electric Ltd.), Ga (5N, Cerac) and Se (5N, Cerac), together with 500 ppmw, 800 ppmw, 900 ppmw, 1000 ppmw, 1550 ppmw, 2000 ppmw or 3000 ppmw Dy^{3+}, added as $DyCl_3$ powder (4N, Sigma-Aldrich) or 3000 ppmw Dy foil, were used to produce the glasses. As, and Se, were further purified by heating under vacuum (10^{-3} Pa) at 300 °C, and 250 °C, prior to batching (8-9 g), which was carried out inside a glove-box (≤ 0.1 ppm O_2, ≤ 0.1 ppm H_2O; MBraun). The silica glass ampoules (< 1.0 ppm OH, ID/OD = 10 mm/14 mm, MultiLab.) in which the glasses were batched and melted, had been air-baked (1000 °C for 6 hours) and vacuum baked (1000 °C for 6 hours at 10^{-3} Pa) prior to use. The ampoule, containing the chalcogenide glass batch, was sealed under vacuum (~10^{-3} Pa) and experienced 96 h rocking at 930°C in a furnace (Instron, TF105/4.5/1ZF) to achieve melt-homogenization. Subsequently the furnace temperature was decreased to 800°C and there was a 2 hours' vertical-dwell for refining. The melt was quenched in situ through the glass transition temperature (T_g) in a liquid metal alloy pot (Seba Developments Ltd.) and the ampoule was then placed into a furnace, preset at the DTA $T_{g,\,onset}$, for annealing for 1h. The furnace was switched off and the ampoule slowly cooled to ambient to make chalcogenide glass rod samples.

2.2.Sample characterisation

The methodologies of characterisation *via* X-ray diffraction (XRD), high resolution transmission electron microscopy (HRTEM), environment scanning electron microscope (ESEM), compositional analysis using energy dispersive X-rays (EDX) and Fourier transform infrared spectroscopy (FTIR) have all been detailed by Tang *et al.* [11,12,20]. The FTIR data presented in [11,12,20] were not on an absolute scale, but the relative intensities of the absorption bands were quantitative. For data comparison, here the minimum absorption level (baseline) of each glass FTIR spectrum has been scaled to match the corresponding minimum absorption level of the host glass. FTIR spectra for

glasses which exhibited low levels of scattering (Ga_{10}:500Cl, Ga_{10}:800Cl and Ga_{10}:3000foil) were vertically shifted to overlay the host glass spectrum at 1.5 µm wavelength. For glasses with evidence in the FTIR spectra of some increased light scattering (Ga_{10}:1000Cl, Ga_{10}:1550Cl, Ga_{10}:2000Cl and Ga_3:3000Cl) the spectral overlay with the host glass was instead at 10.65 µm. The scattering loss for the Ga_{10}:3000Cl sample, which extended from 1 to 16 µm, never approached the lower losses of the host glass so the FTIR spectrum was matched to the host glass at 18.66 µm. By creating these fixed points, any differences in the Dy^{3+} absorption bands may be compared directly as the Dy^{3+} doping levels were increased across the glass series.

2.3.EXAFS experiment

The EXAFS experiment was carried out using the B18 beamline [21] at the Diamond Light Source (Rutherford Appleton Laboratory, Harwell). A thin polished disc (< 8 mm diameter) of each glass was mounted in a sample holder and cooled to ~70K in a liquid nitrogen cooled cryostat. The measurements were performed at the Dy L_3 edge (7790eV), using a double crystal Si111 monochromator and the Pt-coated branch. The energy was scanned from 7600 to 8550 eV (~14 $Å^{-1}$ in k-space) in ~ 1 eV step intervals. Measurements of the glasses were taken in fluorescence mode using a high rate 9 element Ge solid state detector. A Dy_2O_3 (Alfa Aesar 99.99%) standard was measured in transmission using two ionisation chambers to determine the incident and transmitted flux. To ensure an appropriate transmission level, 4 mg of Dy_2O_3 was mixed with 40 mg of cellulose and the powder was pressed into a pellet using an 8 mm diameter die. For the duration of the experiment, the beam current was ~ 240 mA. Glass data were collected for between 8 and 12 hours, depending on the concentration of Dy^{3+} present in the sample, and the quality of the data allowed 2-12 $Å^{-1}$ to be used when fitting the data in k-space. The data were analysed by means of the IFFEFIT suite of programs for EXAFS analysis [22].

3. Results:

3.1.SEM and XRD and TEM

The bulk glass compositions were measured for two glasses, Ga_{10}:500Cl and Ga_{10}:2000Cl, using ESEM-EDX (Table 2) and the measured compositions were found to match the as-batched compositions to ± 1.5 at.%, for all elements. No chlorine was detected in the Ga_{10}:500Cl glass (0.1 at.% expected), and 0.3 at.% Cl was measured in Ga_{10}:2000Cl (0.4 at.% expected). No Dy was detected in Ga_{10}:500Cl (expected 0.02 at%) or Ga_{10}:2000Cl (expected 0.1 at%) due to the low level of Dy present, which was below the detection limits.

Figure 1 shows the XRD patterns collected for all glasses. Note, this is a subsection of previously reported XRD patterns [7,11,12,19,20]. The Ga_{10} glasses doped with < 1000 ppmw Dy^{3+} added as $DyCl_3$ were all X-ray amorphous. The Ga_{10} glasses containing ≥ 1000 ppmw Dy^{3+} as $DyCl_3$ exhibited Bragg diffraction peaks, indexed as α-Ga_2Se_3 [12]. The clear threshold for onset of crystallisation of the as-melted Ga_{10} glasses at 1000 ppmw Dy^{3+} added as $DyCl_3$ is not maintained for Ga_{10}:3000Dyfoil or Ga_3:3000Cl glasses which were X-ray amorphous [12].

HRTEM images, shown in Figure 2, were collected for the Ga_{10}:2000Cl and Ga_3:3000Cl glasses. These results were previously reported by Tang *et al.* [11,12]. Evidence of α-Ga_2Se_3 nanocrystallites were found in both glasses, with those in the Ga_3:3000Cl being between 20-150 nm in diameter, while those in Ga_{10}:2000Cl were ~20-300 nm in diameter. Therefore, although the Ga_3:3000Cl was X-ray amorphous, there were nanocrystallites in the glass, but not of sufficient number, or size, to be observed by X-ray diffraction.

3.2.FTIR

The FTIR measurements shown in Figure 3a, are a subset of those previously published by Tang *et al.* [7,11,12], rescaled to allow direct comparison between samples. The spectra showed little scattering in the wavelength range 1-15 µm for the host glass, Ga_{10}:500Cl, Ga_{10}:800Cl and Ga_{10}:3000foil glasses. When more than 800 ppmw Dy^{3+}, as $DyCl_3$, was doped into the Ga_{10} glass, there was increased scattering at short wavelengths. Furthermore, the wavelength at which the scattering was lowered to the level of the host glass shifted to longer wavelengths with increasing Dy^{3+} content. This shift may be quantified by considering the wavelength at which the scattering of the Dy^{3+} doped glasses fell to three times that of the base glass. This was achieved at 3.0, 4.3, 6.0 and 10.5 µm for the Ga_{10} glasses doped with 1000, 1550, 2000 and 3000 ppmw Dy^{3+} as $DyCl_3$ respectively. The Ga_3:3000Cl glass had scattering losses comparable to the Ga_{10}:1550Cl glass, indicating that the inclusions that caused the scattering were probably present in comparable amounts in these two glasses. Figure 3b shows a more detailed comparison of the Dy^{3+} absorption bands at ~1.1 and 1.3 µm for seven Ga_{10}:Cl glasses (Ga_{10}:1000Cl is not shown because the scattering level for this glass changed too rapidly in the region of interest). The glasses containing ≥ 1000 ppmw Dy^{3+} for the Ga_{10}:Cl series had a structured Dy^{3+} absorption band shape that was absent from the 0-800 Dy^{3+} Ga_{10}:Cl glasses. Figure 3c shows the data for Ga_{10}:3000Cl, Ga_3:3000Cl and Ga_{10}:3000foil glasses. The former two show structured Dy^{3+} absorption bands at 1.1 and 1.3 µm and high scattering losses. In contrast the spectrum of the Ga_{10}:Dyfoil glass has low scattering losses and smooth unstructured Dy^{3+} absorption bands.

3.3.EXAFS

EXAFS (Figure 4a), gave absorption data out to 12 $Å^{-1}$ for all glasses. Figure 4b groups together the spectra to demonstrate that two very different kinds of EXAFS spectra that were collected. EXAFS for Ga_{10}:500Cl, Ga_{10}:800Cl and Ga_{10}:3000foil samples were similar and had symmetric oscillations in k-space that suggested that the data could be fitted as a single shell, having little long range order. In contrast Ga_{10}:1000Cl, Ga_{10}:1550Cl, Ga_{10}:2000Cl, Ga_{10}:3000Cl and Ga_3:3000Cl samples exhibited similar EXAFS spectra that were more complex than those exhibited by the low Cl doped and foil doped glasses, requiring the assumption of more than one shell for fitting. In particular, the peaks at 7.5 and 10.5 $Å^{-1}$ exhibited asymmetry, indicating a more structured Dy^{3+} local environment. In fitting the data, crystal structures for Dy_2Se_3 [23] and $DyCl_3$ [24] were used to generate coordination shells using IFFEFIT [22]. A single Dy-Se bond length was used to fit the EXAFS spectra for Ga_{10}:500Cl, Ga_{10}:800Cl and Ga_{10}:3000foil. Conversely, the glasses containing ≥ 1000 ppmw $DyCl_3$ required 3 contributions for fitting: two Dy-Cl bond lengths and one Dy-Dy bond length. The EXAFS data for Dy_2O_3 were also fitted using crystallographic information [25], and the shells for this model failed to give a good fit to any glass. Due to the hygroscopic nature of crystalline $DyCl_3$, its pure phase EXAFS spectrum could not be obtained.

The Dy-Se bond length (Table 3) for Ga_{10}:500Cl, Ga_{10}:800Cl and Ga_{10}:3000foil (Figure 5), optimised using the IFFEFIT suite of programs [22], was 2.966(7) Å, and coordination numbers extracted from the fits were 7-8. This is consistent with bond valence calculation [26], which indicates that the average bond length of a [$DySe_6$] unit would be 2.92 Å and for a [$DySe_7$] unit would be 2.97 Å. Therefore, in Ga_{10} glasses doped with < 1000 ppmw Dy^{3+} as $DyCl_3$, or doped with 0-3000 ppm Dy foil, the dysprosium local environment appears to be dominated by bonding to Se and it is therefore concluded that the dysprosium had entered the glass network.

As stated above, EXAFS spectra for glasses doped with ≥ 1000 ppmw Dy^{3+} as $DyCl_3$ (Figure 6) required three contributions for fitting. These were taken from the published crystal structure of $DyCl_3$ for fitting, viz.: two Dy-Cl distances (2.659 and 3.17(3) Å) and one Dy-Dy distance (3.99(2) Å). The Dy-Cl coordination numbers were fixed at 6 short and 2 long bonds, and the Dy-Dy coordination number was allowed to vary from a starting number of 6. The resultant fits indicated that the Dy^{3+} was in a distorted $DyCl_3$ environment. The short Dy-Cl bond lengths were similar to those in crystalline $DyCl_3$ [24], but both the long Dy-Cl bonds, and the Dy-Dy distances were each lengthened by ~0.2 Å from those predicted by the $DyCl_3$ crystal structure. While 6 Dy-Cl bonds of length 2.66 Å satisfied the requirements of bond valence [26], the additional two Dy-Cl bonds were found essential to achieve a low R factor for the fit. It should be noted that although the Dy-Dy shell was also required to achieve

a satisfactory R factor for a fit using IFFEFIT [22], the error associated with the coordination numbers of this shell were found to be very large (~40%). We attribute this to the Dy environment being nanocrystalline and highly distorted, reducing the coherence of the interference patterns arising from the Dy-Dy shell.

4. Discussion

$DyCl_3$ has the advantage of being readily available and easy to batch into the glass in powder form, but is hygroscopic and must be handled in a water free environment (for instance during all glass batching it was stored and used in an MBraun glovebox of ≤ 0.1 ppm H_2O). Dy metal is oxidised under ambient conditions and can be discoloured, even when stored in a glovebox (≤ 0.1 ppm O_2). As a result, the large surface area of Dy foil can introduce significant impurity levels to chalcogenide melts. $DyCl_3$ has the potential to introduce fewer impurities to the glass and remove any hydrogen impurities present through the evolution of $HCl_{(g)}$ (gas) during glass-melting. This study was, in part, undertaken to investigate the effect of using $DyCl_3$ as the precursor for rare earth doping into chalcogenide glass.

4.1.Composition of the glasses

ESEM-EDX compositional analysis of the glasses (Table 2) showed no evidence of Cl in the Ga_{10}:500Cl glass, suggesting that either the amount of chlorine was below the detection limit of the equipment, or that all chlorine had been removed from the glass during melting as $HCl_{(g)}$ (see preceding paragraph). In contrast, chlorine was measured in the Ga_{10}:2000Cl glass at a level consistent with that added by the precursor. The concentrations of the Ge, Ga and Se in Ga_{10}:500Cl and Ga_{10}:2000Cl glasses, according the ESEM-EDX, deviated from those expected by more than the $\pm$ 0.5 at.% errors expected of the analysis software, yet always by < 1.5 at.%. For Ga_{10}:500Cl and Ga_{10}:2000Cl, the measured concentrations of As and Se were lower than expected, whereas the measured concentrations of Ga and Ge were higher than expected. It is known that As and Se can evaporate during the melt, depositing on the walls of the containment ampoule and so be lost to the glass melt. However, as no independent calibration measurements were made, and given the mass dependence in the deviation from nominal compositions, it is suggested that these differences are of the order that might be expected when using an automatic calibration for four elements and that there was no significant variation in the bulk glass composition from nominal.

4.2. XRD, FTIR and HRTEM results

The XRD data (Figure 1) revealed Bragg peaks (indexed as α-Ga_2Se_3 crystallites [12]) in Ga_{10} glasses doped with ≥1000 ppmw $DyCl_3$. The undulating background indicated that much amorphous material was still present. Neither Ga_3:3000Cl nor Ga_{10}:3000foil, exhibited Bragg peaks. It is

concluded that X-ray observable α-Ga_2Se_3 crystallites occurred only at high gallium and high $DyCl_3$ concentrations. The Bragg peak intensity of Ga_{10}:1000-3000Cl increased with Dy^{3+}, and peak narrowing occurred up to ~2000 ppmw $DyCl_3$, then plateaued [12]. Dy^{3+} has been proposed to heterogeneously nucleate α-Ga_2Se_3 [11].

Four of the FTIR spectra (Figure 3) exhibit low baseline loss from 1-14 μm, with smooth Dy^{3+} absorption bands, where present. Four of the FTIR spectra (Figure 3) for Ga:≥1000Cl have high scattering loss and sharp, structured Dy^{3+} absorption bands, indicating a more crystalline Dy^{3+} local environment. Direct comparison of the XRD patterns (Figure 1) with the FTIR spectra (Figure 3) shows correlation of X-ray amorphicity with low scattering losses and smooth Dy^{3+} absorption bands and, conversely, X-ray Bragg peaks due to α-Ga_2Se_3 with high scattering loss and structured Dy^{3+} absorption bands. The only anomalous glass bucking this trend was Ga_3:3000Cl. This glass exhibited high scattering loss and structured bands in FTIR, but no Bragg peaks in the XRD pattern. However, although X-ray amorphous, HRTEM does show that it contained α-Ga_2Se_3 nanocrystallites (Figure 2). The results suggest a link between the presence of both crystalline Dy^{3+} and α-Ga_2Se_3 crystals and scattering loss. It has previously been noted that the threshold for scattering from α-Ga_2Se_3 in this glass matrix is significantly higher than Dy-containing crystallites, based on the refractive index difference of the scattering centre and the matrix, making the latter one of the dominant scatterers in the glass [11]. This suggestion is supported by the plateau in intensity of the α-Ga_2Se_3 Bragg X-ray peaks for > Ga_{10}:2000Cl, yet concomitant increase in FTIR scattering. Nevertheless, it is clear that for the Ga_{10} series below 1000 ppmw Dy^{3+} there is no evidence of crystallisation and above 1000 ppmw Dy^{3+} both Ga and Dy^{3+} adopt more ordered crystalline environments. A more detailed analysis, [12], has indicated that α-Ga_2Se_3, when present in the Ge-As-Ga-Se RE-ion doped glasses, has a low level of Ge substitution onto Ga sites. As there has been no evidence to date of a germanium selenide crystal phase forming when there is insufficient Ga, the observed relationship between $DyCl_3$ content and the formation of crystallites from the bulk glass constituents is proposed to be limited to Dy^{3+} and Ga^{III}. The electropositive RE ion has been widely proposed as attracted to negatively charged [$GaSe_4$] units in the glass, accounting for the enhanced solubility and fluorescent intensity of rare earth ions in Ga-containing chalcogenide glasses [14,15,17,27]. We have found no evidence of crystallisation of α-Ga_2Se_3 in Ga_3 or Ga_{10} as-annealed glasses up to 6000 ppmw Dy^{3+} for glass doped with Dy foil on melt-quenching [28], and so the presence of chlorine is a key factor. Work by Cheng *et al*. [28] investigated isothermal heat treatment at fibre drawing temperatures, of a series of Ga_3:Dyfoil glasses. Under these conditions of high temperature heat treatment, α-Ga_2Se_3 grew in both doped and undoped glasses, yet this phase growth diminished as the Dy^{3+} dopant level was increased, in contrast to the results for melt-quenched $DyCl_3$ glasses, where an increase in Dy^{3+}

content encouraged the α-Ga_2Se_3 crystal growth. This is further evidence of the strong interdependence between Dy^{3+} and Ga^{III}, with Dy^{3+} alone (added as foil) acting to stabilise the glass matrix on heat-treating at elevated temperature, yet the presence of chlorine encouraging crystal growth on melt-cooling.

4.3. The local environment of Dy^{3+} determined by EXAFS

To the Authors' knowledge, this is the first investigation of the RE ion environment in selenide glasses. In a series of Ge-As-Ga-Se glasses doped with $DyCl_3$ doped or Dy foil, two different local environments for Dy^{3+} were identified using EXAFS (Figure 4). First Dy^{3+} bonded to selenium in an amorphous local structure, and second as Dy^{3+} bonded to chlorine in a crystalline local structure. Figure 5 shows fitting to a single Dy-Se shell at ~2.97 Å of Ga_{10}:500Cl, Ga_{10}:800Cl and Ga_{10}:3000foil; these glasses also exhibiting smooth amorphous Dy^{3+} absorption bands in the FTIR spectra, interpreted also as an amorphous local Dy^{3+} environment. Note that the coordination numbers here were found to be 7-8, in agreement with the RE ion coordination numbers found for sulfides [16-18]. In direct contrast, EXAFS here of Ga: ≥1000Cl glasses (Figure 6, Table 3) indicated Dy^{3+} ions in a nanocrystalline chloride environment, and FTIR likewise exhibited structured Dy^{3+} absorption bands. Heo [17], showed that as CsBr was added to a Tm doped GeGaS glass, Tm-Br bonds dominated the EXAFS spectra, yet Tm-S bonds prevailed in the absence of CsBr. Importantly, Heo [17] also reported the first direct indication that RE ions can be spatially correlated with Ga, fitting the Ga K edge EXAFS spectra with a mix of Ga-Se and Ga-Br bonds.

Aitken *et al*. [14] demonstrated that to maximise fluorescence, it is necessary to have ≥ 10 Ga^{III} atoms to 1 RE ion. Here a Ga^{III}:RE ratio > 20 was preserved (Table 1), so one might expect that the RE ions would have been evenly distributed throughout the glass network, yet we found a substantive change in Dy^{3+} environment at 1000 ppmw $DyCl_3$, no matter if doped into Ga_{10} or Ga_3 glasses [11]. This suggests that the local environment change of Dy^{3+} is not in fact related to the Ga^{III}:Dy^{3+} ratio. Rather it may be related to retention of Cl in the glass, instead of loss as $HCl_{(g)}$ during glass melting. $TeCl_4$ is a popular hydrogen-getter for purifying chalcogenide glass melts. These results suggest its use may in fact lead to Cl retention, binding to RE-ions and thereby adversely affecting RE ion emission behaviour.

$DyCl_3$ has been demonstrated to attack the SiO_2 chalcogenide melt containment ampoule more aggressively that Dy foil, introducing Si, Dy and O into the outer surface of Ge-As-Ga-Se glasses [20,29] as, possibly, Dy_2O_3 or Dy-O-Si species [20,29]. In their work, Tang *et al.* have failed to detect Dy^{3+} using SEM-EDX in Ga_3 and Ga_{10} glasses doped with $DyCl_3$ or Dy foil. Careful work by Tang *et al.* using HRTEM showed one sighting of raised atomic % of Dy and O in the presence of α-Ga_2Se_3 in the

bulk Ga_3:3000Cl glass [11]. In this regard, it is important to note that EXAFS has failed to reveal Dy-O units in any of the glasses analysed here, and this lends weight to Dy_2O_3, if it exists, being a minority bulk phase. Rather, it is concluded here that for Ga_{10}:≥1000Cl glasses, $DyCl_3$ is the primary nucleation catalyst for α-Ga_2Se_3 crystallites in Dy^{3+}-doped GeAsGaSe glasses. For the Ga_{10}:500Cl, Ga_{10}:800Cl and Ga_{10}:3000foil glasses it is encouraging to note that evidence here from FTIR, XRD and EXAFS combine to suggest that the first coordination sphere consists of 7-8 Dy-Se bonds, meaning that the RE-ion is in the optimum low phonon energy environment for efficient fluorescence and RE-doped selenide chalcogenide glasses are an attractive proposition for mid-IR fibre lasing.

5. Conclusions

EXAFS measurements on Dy^{3+}-doped GeAsGaSe glasses, together with FTIR and XRD and HRTEM, lead to a clear and unambigious picture of the variation in Dy^{3+} environment with composition. For glasses doped with Dy metal foil or < 1000 ppmw $DyCl_3$, Dy^{3+} enters the glass network with a first coordination sphere of 7-8 bonds to Se, conducive to efficient radiative transitions. However, when ≥ 1000 ppmw $DyCl_3$ is doped into the glass, Dy^{3+} remains in a distorted crystalline $DyCl_3$ environment. It is concluded that $DyCl^{3+}$ is not a suitable precursor for introducing high concentrations of RE-ions into selenide chalcogenide glasses. The presence of $DyCl_3$ crystallites in the glass necessarily means that the Dy^{3+} ions are spatially clustered; but with this type of clustering it does not necessarily follow that there would be a reducing ability for the ions to fluoresce efficiently. This will be the subject of future work. The increased light scattering from these crystallites compromises glass transmission. Finally, it is proposed that, $DyCl_3$ crystallites act as a nucleating catalyst for α-Ga_2Se_3 reducing the glass stability.

Tables

Table 1: The nominal glass batch compositions and the relative atomic ratio of Ga to Dy^{3+} in each glass. Code names for the glass are also given. Key: ppmw is parts per million by weight.

Nominal concentration of Dy^{3+}	At.% Dy^{3+}	Ga/Dy^{3+}	Code
0 ppmw Dy^{3+} in Ga_{10}	**0**	**N/A**	**host glass**
500 ppmw Dy^{3+} ($DyCl_3$) in Ga_{10}	**0.024**	**416.57**	**Ga_{10}:500Cl**
800 ppmw Dy^{3+} ($DyCl_3$) in Ga_{10}	**0.038**	**263.10**	**Ga_{10}:800Cl**
1000 ppmw Dy^{3+} ($DyCl_3$) in Ga_{10}	**0.047**	**212.72**	**Ga_{10}:1000Cl**
1550 ppmw Dy^{3+} ($DyCl_3$) in Ga_{10}	**0.073**	**136.95**	**Ga_{10}:1550Cl**
2000 ppmw Dy^{3+} ($DyCl_3$) in Ga_{10}	**0.094**	**106.36**	**Ga_{10}:2000Cl**
3000 ppmw Dy^{3+} ($DyCl_3$) in Ga_{10}	**0.141**	**70.91**	**Ga_{10}:3000Cl**
3000 ppmw Dy^{3+} (Dy foil) in Ga_{10}	**0.141**	**70.91**	**Ga_{10}:3000foil**
3000 ppmw Dy^{3+} ($DyCl_3$) in Ga_3	**0.142**	**21.27**	**Ga_3:3000Cl**

Table 2: The glass compositional analysis for Ga_{10}:500Cl and Ga_{10}:2000Cl, carried out using ESEM-EDX.

	Nominal 500 ppmw Dy^{3+}		Nominal 2000 ppmw Dy^{3+}	
Element	**nominal (at.%)**	**measured (at.%)**	**nominal (at.%)**	**measured (at.%)**
Cl	0.1	0.0	0.3	0.4(1)
Ge	16.5	17.5(5)	16.4	16.9(5)
As	10.0	9.1(5)	10.0	9.0(5)
Ga	9.0	10.3(5)	9.0	11.0(5)
Se	64.4	63.0(5)	64.2	62.7(5)

Table 3: The type, number, length and thermal vibrations of dysprosium bonds, as determined by EXAFS. Values with no error (in brackets) were fixed for the refinement.

Composition	R factor of fit	Energy shift	n_{Dy-Cl1}	r_{Dy-Cl1} (Å)	σ_{Dy-Cl1} (Å^2)	n_{Dy-Cl2}	r_{Dy-Cl2} (Å)	σ_{Dy-Cl2} (Å^2)	n_{Dy-Dy}	r_{Dy-Dy} (Å)	σ_{Dy-Dy} (Å^2)
Ga_{10}:3000Cl	0.014	3.5(4)	6	2.659	0.003(1)	2	3.18(2)	0.005(3)	7(3)	3.99(2)	0.008(4)
Ga_{10}:2000Cl	0.015	3.3(4)	6	2.659	0.004(1)	2	3.18(3)	0.007(4)	7(3)	3.99(2)	0.008(4)
Ga_{10}:1550Cl	0.028	3.1(5)	6	2.659	0.005(1)	2	3.17(2)	0.004(3)	7(5)	3.99(3)	0.010(7)
Ga_{10}:1000Cl	0.037	2.4(7)	6	2.659	0.007(1)	2	3.17(3)	0.006(4)		3.98(3)	
Ga_3:3000Cl	0.020	2.2(5)	6	2.659	0.006(1)	2	3.14(3)	0.008(4)		4.01(4)	
			n_{Dy-Se}	r_{Dy-Se} (Å)	σ_{Dy-Se} (Å^2)						
Ga_{10}:800Cl	0.022	2.0(9)	8(1)	2.966(7)	0.007(1)						
Ga_{10}:500Cl	0.022	2.0(9)	7(1)	2.966(6)	0.007(1)						
Ga_{10}:3000foil	0.022	2.0(9)	7(1)	2.966(7)	0.007(1)						

Figures

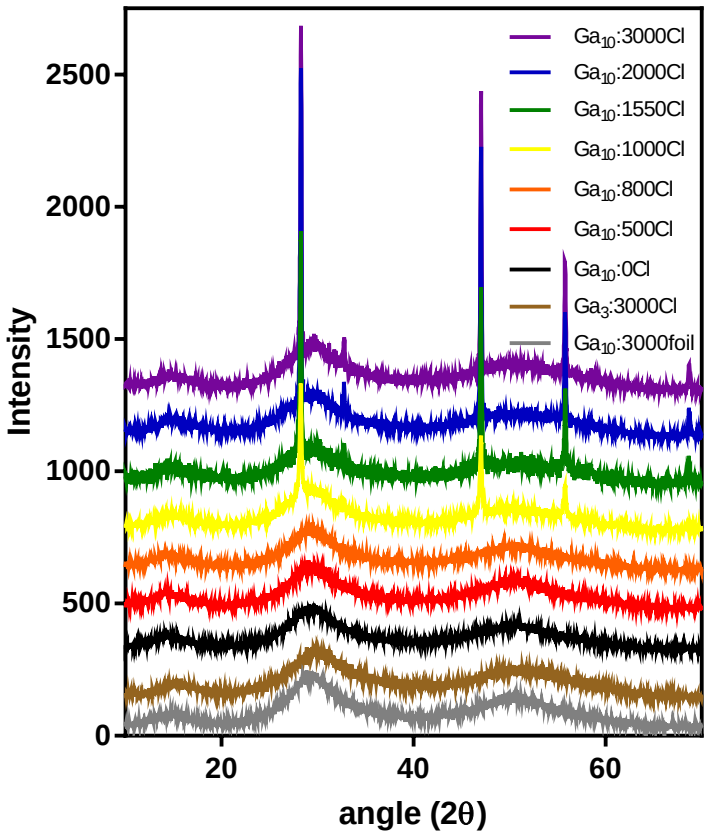

Figure 1: X-ray diffraction patterns measured for nine glasses of composition $Ge_{16.5}As_9Ga_{10}Se_{64.5}$(at%) doped with 0 to 3000 ppmw Dy^{3+} [7,11,12,19,20]. The X-ray patterns are offset on the y-axis for clarity.

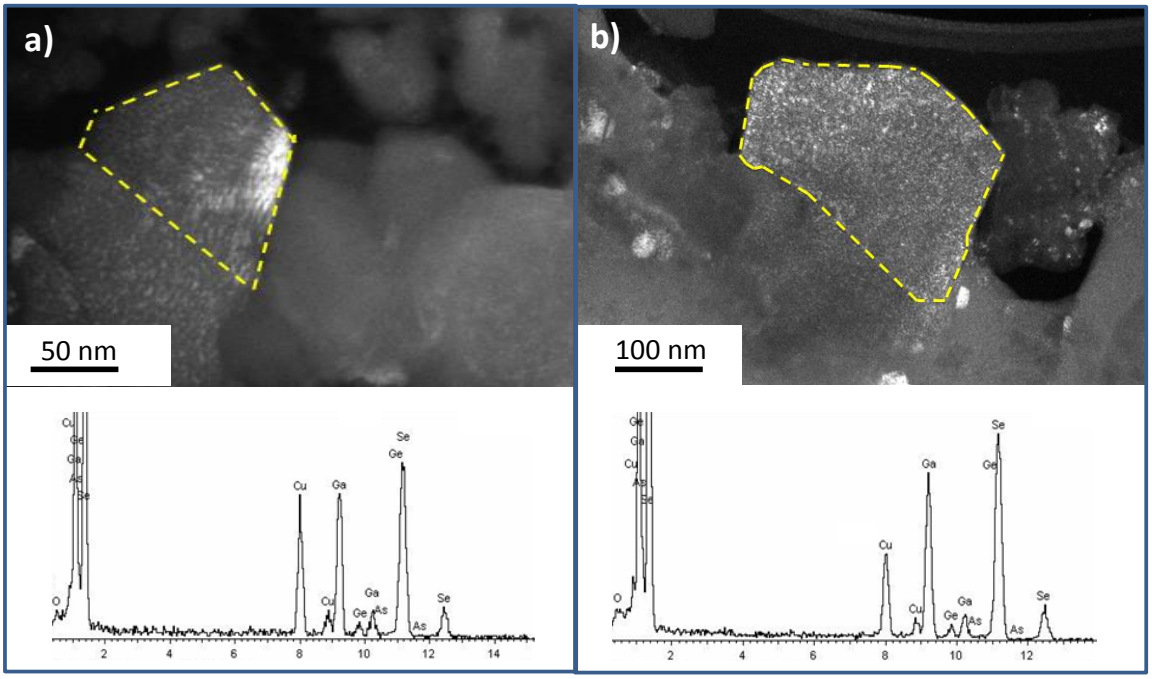

Figure 2: HRTEM images for: a) Ga_3:3000Cl [11] and b) Ga_{10}:2000Cl [12], with an α-Ga_2Se_3 crystal highlighted (yellow dashed line). The elemental analysis of the crystal phase is also shown [11].

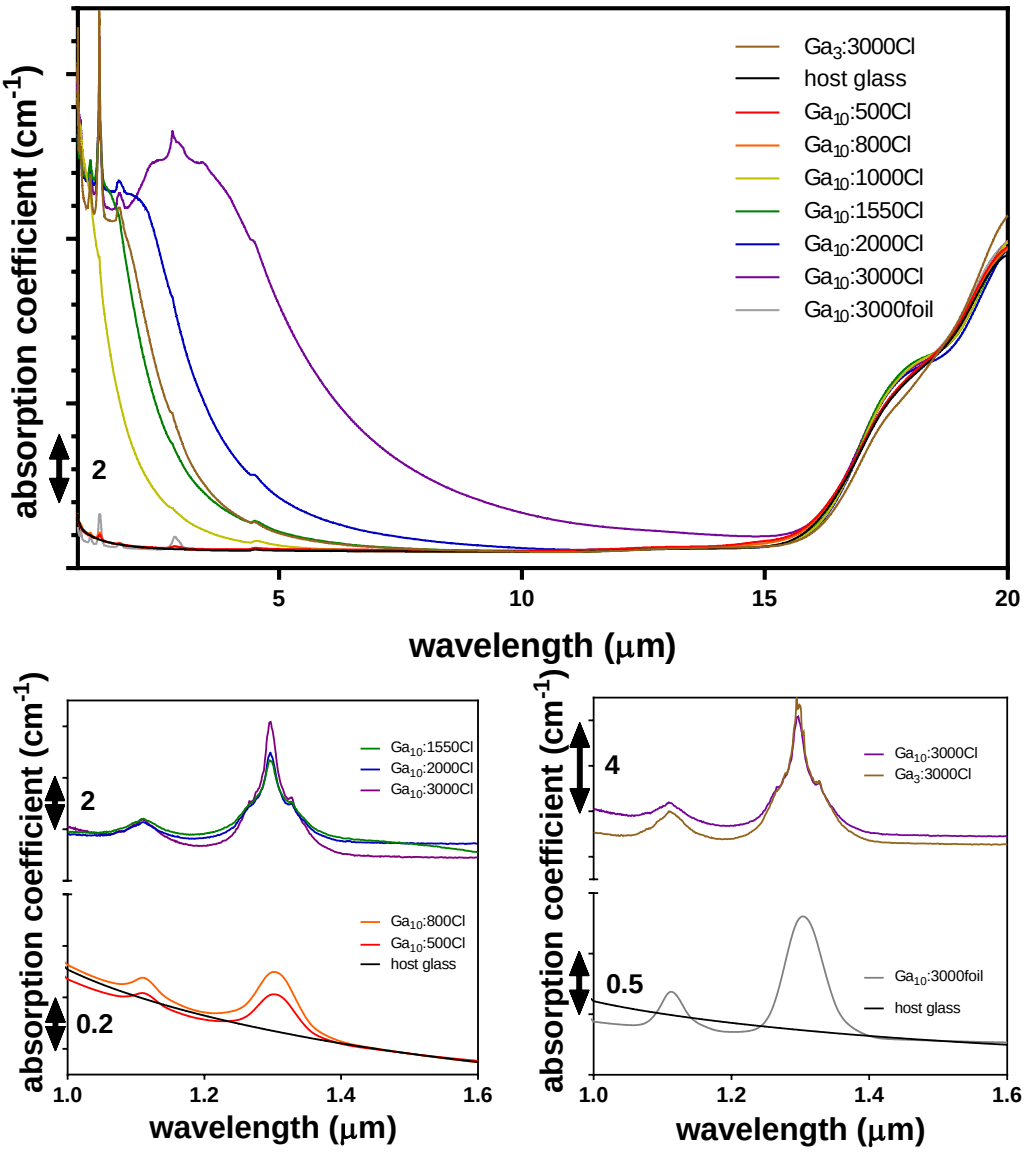

Figure 3: a) FTIR spectra for the ten glass samples (some previously reported in [7,11,12]), doped with 0 to 3000 ppmw Dy^{3+} as both $DyCl_3$ and foil. The samples were of the same optical path length = 2.238±0.005 mm. The absorption-bands at shorter wavelength correspond to the electronic absorption of Dy^{3+}. Figures b) and c) show the Dy^{3+} electronic absorption bands at ~1.1 and 1.3 μm for the glass series doped with: b) $DyCl_3$ and c) 3000 ppmw Dy^{3+} as $DyCl_3$ or Dy foil into Ga_3 and Ga_{10} host glasses.

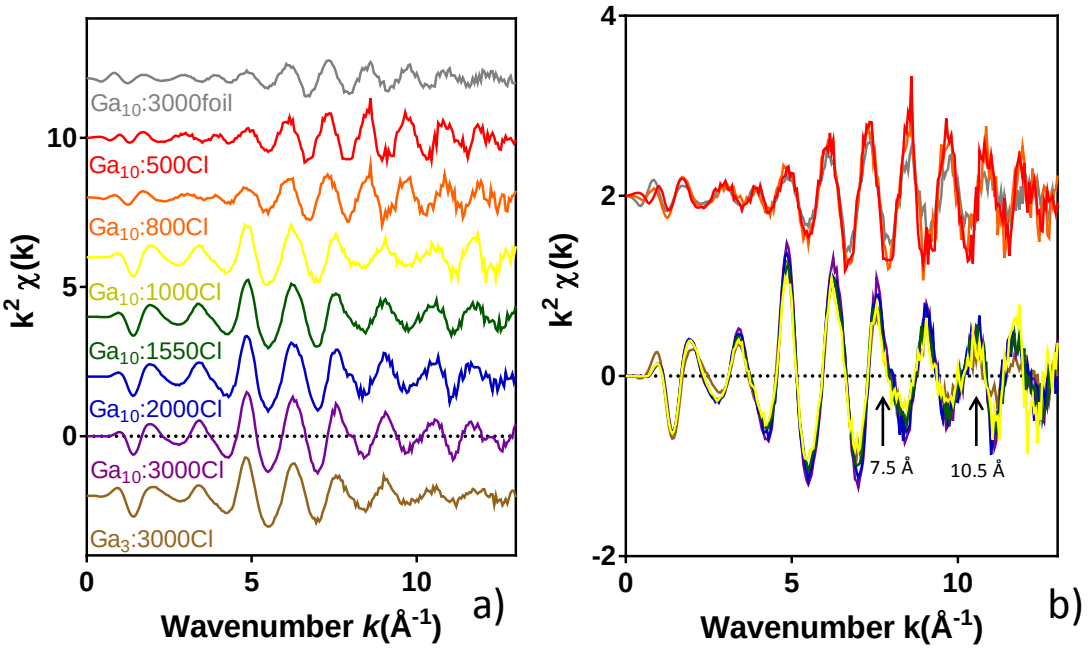

Figure 4: a) The k^2 EXAFS data for each of the 10 Dy^{3+} doped glasses. The spectra are plotted with offsets for clarity. b) the two different oscillation patterns are grouped together. The Ga_{10}:3000foil, Ga_{10}:500Cl and Ga10:800Cl are offset by 2 on the y axis, and all the remaining spectra are plotted without a shift applied. The asymmetric oscillations at 7.5 and 10.5 Å in spectra for glasses containing ≥1000 ppmw Dy^{3+}, added as $DyCl_3$, are labelled.

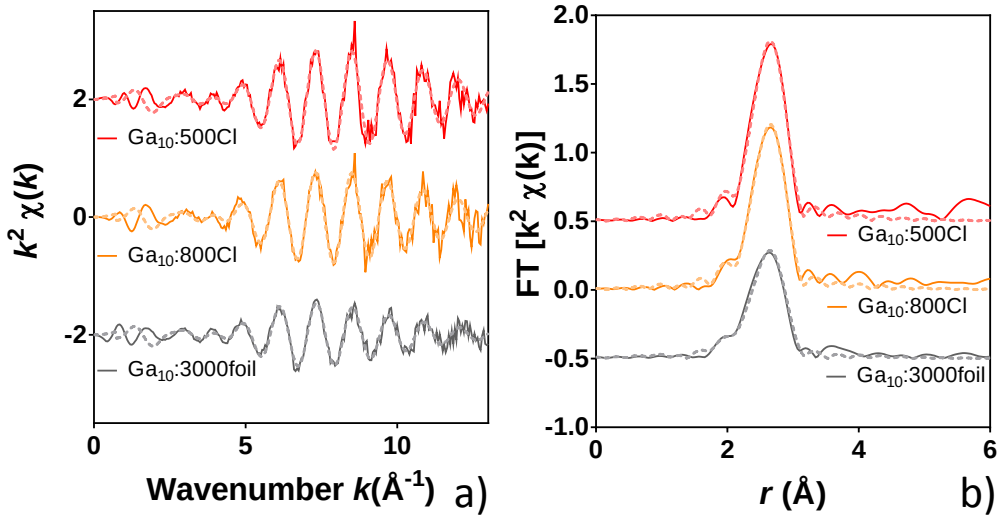

Figure 5: EXAFS fits in: a) k^2 and b) real space, for the Ga_{10}:3000foil, Ga_{10}:500Cl and Ga_{10}:800Cl glasses. Experimental data are shown with a solid line and dashed lines show the fit.

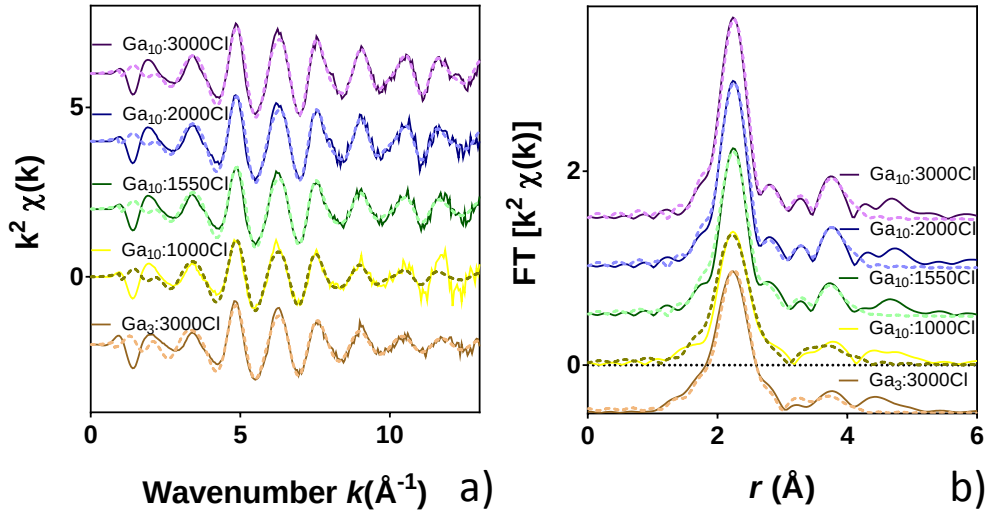

Figure 6: EXAFS fits in: a) k^2 and b) real space, for the Ga_{10}:1000Cl, Ga_{10}:1550Cl, Ga_{10}:2000Cl, Ga_{10}:3000Cl, and Ga_3:3000Cl glasses. Experimental data are shown with a solid line and dashed lines show the fit.

References

[1] L.J. Medhurst, Journal of Chemical Education, 82 (2005) 278.
[2] B. Van Eerdenbrugh, L.S. Taylor, Int. J. Pharm., 417 (2011) 3.
[3] L.M. McIntosh, M. Jackson, H.H. Mantsch, M.F. Stranc, D. Pilavdzic, A.N. Crowson, J. Invest. Dermatol., 112 (1999) 951.
[4] D.J. Richardson, J. Nilsson, W.A. Clarkson, J. Opt. Soc. Am. B, 27 (2010) B63.
[5] M. Bernier, V. Fortin, M. El-Amraoui, Y. Messaddeq, R. Vallée, Opt. Lett., 39 (2014) 2052.
[6] D. Hudson, E. Magi, L. Gomes, S.D. Jackson, Electron. Lett., 47 (2011) 985.
[7] A.B. Seddon, Z. Tang, D. Furniss, S. Sujecki, T.M. Benson, Opt. Express, 18 (2010) 26704.
[8] S. Danto, D. Thompson, P. Wachtel, J.D. Musgraves, K. Richardson, B. Giroire, International Journal of Applied Glass Science, 4 (2013) 31.
[9] V.S. Shiryaev, M.F. Churbanov, J. Non-Cryst. Solids, 377 (2013) 225.
[10] J.S. Sanghera, I.D. Aggarwal, J. Non-Cryst. Solids, 213–214 (1997) 63.
[11] Z.Q. Tang, D. Furniss, M. Fay, N.C. Neate, Y. Cheng, E. Barney, L. Sojka, S. Sujecki, T.M. Benson, A.B. Seddon, J. Am. Ceram. Soc., 97 (2014) 432.
[12] Z.Q. Tang, N.C. Neate, D. Furniss, S. Sujecki, T.M. Benson, A.B. Seddon, Journal of Non-Crystalline Solids, 357 (2011) 2453.
[13] J.D. Shephard, R.I. Kangley, R.J. Hand, D. Furniss, A.B. Seddon, Phys. Chem. Glasses, 44 (2003) 267.
[14] B.G. Aitken, C.W. Ponader, R.S. Quimby, C R Chim., 5 (2002) 865.
[15] T.H. Lee, S.I. Simdyankin, J. Hegedus, J. Heo, S.R. Elliott, Phys. Rev. B, 81 (2010) 104204.
[16] Y.G. Choi, J.H. Song, Y.B. Shin, J. Heo, J. Non-Cryst. Solids, 353 (2007) 1665.
[17] J. Heo, J. Non-Cryst. Solids, 353 (2007) 1358.
[18] J.H. Song, Y.G. Choi, K. Kadono, K. Fukumi, H. Kageyama, J. Heo, J. Non-Cryst. Solids, 353 (2007) 1251.
[19] Z.Q. Tang, D. Furniss, S. Sujecki, T.M. Benson, A.B. Seddon, in: W.A. Clarkson, N. Hodgson, R. Shori (Eds.), Solid State Lasers Xx: Technology and Devices, 2011.
[20] Z. Tang, D. Furniss, N.C. Neate, T.M. Benson, A.B. Seddon, In preparation, (2014).
[21] A.J. Dent, G. Cibin, S. Ramos, A.D. Smith, S.M. Scott, L. Varandas, M.R. Pearson, N.A. Krumpa, C.P. Jones, P.E. Robbins, 14th International Conference on X-Ray Absorption Fine Structure (Xafs14), Proceedings, 190 (2009).
[22] B. Ravel, M. Newville, J. Synchrotron Rad., 12 (2005) 537.
[23] K.J. Range, R. Leeb, Z Naturforsch B, 31 (1976) 685.
[24] D. Hake, W. Urland, Z. Anorg. Allg. Chem., 586 (1990) 99.
[25] B. Antic, P. Oennerud, D. Rodic, R. Tellgren, Powder Diffraction, 8 (1993) 216.
[26] N.E. Brese, M. O'Keeffe, Acta Cryst. B, 47 (1991) 192.
[27] J. Heo, J. Min Yoon, S.-Y. Ryou, J. Non-Cryst. Solids, 238 (1998) 115.
[28] Y. Cheng, Z. Tang, N.C. Neate, D. Furniss, T.M. Benson, A.B. Seddon, J. Am. Ceram. Soc., 95 (2012) 3834.
[29] Z. Tang, PhD thesis, University of Nottingham, 2013.